

## U-Pb and Rb-Sr Radiometric Dates and their Correlation with Metamorphic Events in the Granulite-Facies Basement of the Serre, Southern Calabria (Italy)

Volker Schenk

Institut für Mineralogie der Ruhr-Universität, Postfach 102148, D-4630 Bochum, Federal Republic of Germany

**Abstract.** An approximately 7 km thick, continuous sequence of granulite-facies rocks from the lower crust, which contains a lower granulite-pyroxene unit and an upper metapelite unit, occurs in the NW Serre of the Calabrian massif. The lower crustal section is overlain by a succession of plutonic rocks consisting of blastomylonitic quartz diorite, tonalite, and granite, and is underlain by phyllonitic schists and gneisses.

Discordant apparent zircon ages, obtained from granulites and aluminous paragneisses, indicate a minimum age of about 1,900 m.y. for the oldest zircon populations. The lower intersection point of the discordia with the concordia at  $296 \pm 2$  m.y. is also marked by concordant monazites. Therefore, the age of  $296 \pm 2$  m.y. is interpreted as the minimum age of granulite-facies metamorphism.

Concordant zircon ages were obtained from a metamorphic quartz monzogabbro sill ( $298 \pm 5$  m.y.) and an unmetamorphosed tonalite ( $295 \pm 2$  m.y.); they are interpreted as the intrusion ages.

Discordant zircon ages from a blastomylonitic quartz diorite gneiss, situated between the lower crustal unit and the non-metamorphosed tonalite, reveal recent or geologically young lead loss by diffusion. The  $^{207}\text{Pb}/^{206}\text{Pb}$  ages of the two analysed size-fractions point to an intrusion age similar to that of the overlying tonalite.

Rb-Sr mineral ages are younger in the granulite-pyroxene unit than in the overlying metapelite unit. Feldspars from the granulite-pyroxene unit yield ages of about 145 m.y. and those from the metapelite unit  $176 \pm 5$  m.y. In the same way, the biotite cooling ages range between 108 and 114 m.y. in the granulite-pyroxene and between 132 and 135 m.y. in the metapelite unit and the tonalite. Some still younger biotite ages are explained by the influence of tectonic shearing on the Rb-Sr systems. A muscovite from a post-metamorphic aplite in the metapelite unit yields a cooling age of  $203 \pm 4$  m.y.

The Rb-Sr isotopic analyses from migmatite bands

do not lie on an isochron, perhaps due to limited isotopic exchange between the small scale layers during the long cooling period after the peak of metamorphism.

In the phyllonitic gneisses and schists a Hercynian metamorphism is indicated by a muscovite age of  $268 \pm 4$  m.y., whereas the biotite age of  $43 \pm 1$  m.y. from the same sample can be correlated with an Alpine greenschist-facies metamorphism.

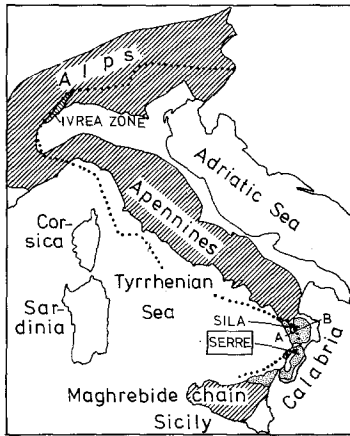
On the basis of the radiometric dates and of the *P-T* path of the lower crustal section deduced petrologically, the following model is presented: the end of the Hercynian granulite-facies metamorphism was accompanied by an uplift of the lower crustal rocks into intermediate crustal levels and by synchronous plutonic intrusions into the lower crust and higher crustal levels, but essentially into the latter. Substantial further uplift did not occur until after cooling from the temperature of the granulite-facies metamorphism to the biotite closing temperature. This cooling lasted for about 185 m.y. in the lower part and for about 160 m.y. in the upper part of the lower crust section.

A comparison between the geologic evolutions of the NW Serre of Calabria and the Ivrea Zone of the Alps demonstrates striking similarities. The activity of deep seated faults in both areas at least since late Hercynian time raises the possibility that a fault precursor of the boundary of the Adriatic microplate already existed at this time.

### 1. Introduction

#### 1.1. Geological Setting

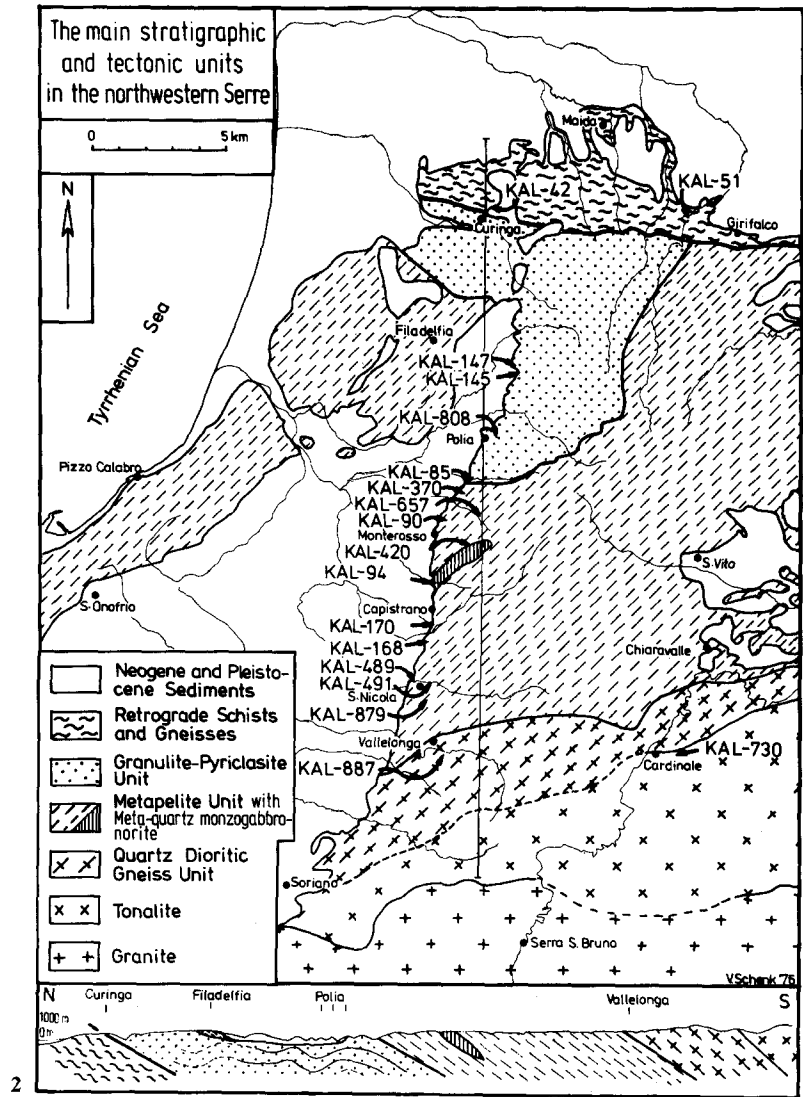
Calabria is situated in the sharp bend connecting the NW-SE Apennine and the W-E Maghrebide Mountain chains of Sicily and Northern Africa (Fig. 1). The extensive exposures of deep continental crust in Calabria are unusual within the Apennine-Maghre-



1

Fig. 1. Location of the Serre in the Calabrian massif (stippled) and of the Ivrea Zone and approximate position of the boundary (dotted line) of the Adriatic microplate (after Giese and Reutter 1978)

Fig. 2. Simplified geological map of the northwestern Serre with the sample locations (numbers). The border between the quartz dioritic gneisses and the tonalite is from the geological map 1:25,000 of Calabria (Cassa per il mezzogiorno). The border tonalite-granite is from Amodio-Morelli et al. (in press)



2

bide system. In the NW Serre, Southern Calabria, granulite-facies rocks are exposed for about 400 km<sup>2</sup> (Fig. 2). The lithostratigraphic sequence exposed (bottom to top) from north to south is (Schenk 1978):

1. Retrograde schists and gneisses (greenschist facies)
2. Granulite-facies rocks of the lower crust
  - (a) Granulite-pyriclasite unit;
  - (b) Metapelite unit;
3. Blastomylonitic quartz dioritic gneisses
4. Tonalite
5. Granite.

Further to the southeast, the granite is overlain by partly contact-metamorphosed phyllites of palaeozoic age which are themselves discordantly overlain by Mesozoic limestones, Tertiary sandstones, and conglomerates (Quitow 1935).

The granulite-facies rocks are separated from the underlying and overlying units by tectonic contacts. The lower contact with retrograde schists and gneisses is a mylonitic fault zone, while at the upper contact the granulitic rocks are interdigitated with blastomylonitic quartz dioritic gneisses.

The two granulite-facies units form an approximately 7 km thick sequence which may represent a continuous section of a former lower crust. The granulite-pyriclasite unit consists predominantly of granulites and pyriclasites with less abundant pyroblites and ultramafic lenses. The metapelite unit, which overlies structurally concordantly but stratigraphically discordantly the granulite-pyriclasite unit, includes predominantly aluminous paragneisses, granofelses, pyriclasites and minor silicate marbles. Also present is a 200–300 m thick metamorphosed sill of

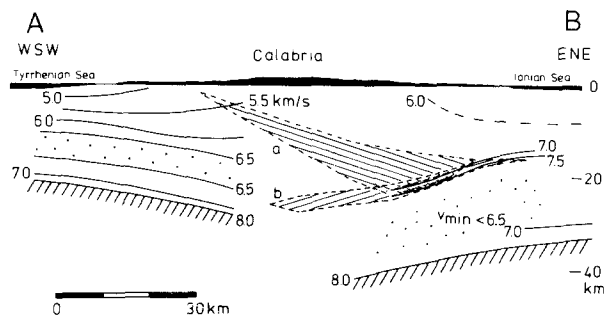


Fig. 3. Two possible crustal structures of Northern Calabria according to two-dimensional computations on the basis of magnetic and seismic data (Schwarz 1978). Crustal structure (lines of equal velocity) after Schütte (1978). Location of the profile (A-B) in Fig. 1

quartz monzogabbriorite and smaller lenses of meta-alkalic granite. The entire sequence exhibits the same granulite-facies metamorphism and post-metamorphic history. Granulite-facies metamorphism occurred in the granulite-pyroxenite unit near 800°C and 8 kb, which corresponds to a depth of about 30 km; it was followed by an isothermal pressure decrease of 1.5–2.0 kb after which cooling occurred at constant pressure or accompanied by a small pressure decrease (Schenk 1977, 1978). The retrograde hydration and amphibolite-facies overprint increase towards the top of the sequence.

The crustal structure beneath Calabria displays some characteristic features. Geophysical investigations have revealed a crustal doubling due to subduction of the Adria microplate beneath the Tyrrhenian crust; this crustal doubling is common along the border of the Adria microplate (Giese and Reutter 1978). In addition, a high velocity layer was detected under the Sila (Northern Calabria) at a depth of about 20 km and this is underlain by a velocity inversion, thereby indicating a crust-mantle boundary inside the subducted Adria plate (Schütte 1978). According to the two-dimensional model computations based on magnetic measurements and seismic data in the Sila (Schwarz 1978), a connection between the lower crustal rocks at the surface and the high velocity layer at depth is possible (Fig. 3). Gravimetric data in Southern Calabria are compatible with an analogous crustal structure in this area, although corresponding seismic data are still lacking (Giese and Reutter 1978).

The crustal structure of Calabria as determined by the geophysical investigations as well as the geologic and petrologic features of the NW Serre show remarkable similarities with the Ivrea Zone of the Alps (Schenk and Schreyer 1978). This supports modern reconstructions of the geological history of the central Mediterranean in which Calabria is interpreted as a former continuation of the Alps. The rocks of the

lower crust in the Sila and the Serre are thought to have been originally part of the African shelf split off during early Alpine phases (Haccard et al. 1972; Alvarez 1976; Görler and Giese 1978; Amodio-Morelli et al., in press). On the other hand, the author pointed out, on the basis of his petrological work (Schenk 1978), resemblances between the Serre and the Moldanubicum in the Central European Hercynian belt where relatively small granulite bodies with the characteristic rock association of fine-grained granulites, pyroxenites, and ultramafics are linked with anatectic paragneiss series as in the Serre. This may support a former connection of the Calabrian basement with the Hercynian belt of central Europe in Palaeozoic time.

### 1.2. Previous Geochronological Studies and Purpose of this Work

Geochronological studies have addressed the age of the granites, granulite-facies rocks, and greenschist metamorphism. The granites of the Serre and the Sila have late-Hercynian cooling ages of 230<sup>1</sup> to 295<sup>1</sup> m.y., according to Rb-Sr determinations on biotites (Ferrara and Longinelli 1961; Borsi and Dubois 1968; Borsi et al. 1976). The Rb-Sr biotite ages in the granulite-facies rocks and in the tectonically overlying quartz dioritic gneisses and tonalite range between 152<sup>1</sup> and 132<sup>1</sup> m.y. (Borsi et al. 1976). Borsi et al. propose to relate these dates either with a metamorphic event or preferably with the cooling during an early Alpine uplift. The greenschist-facies overprint in the retrograde schists and gneisses which underlie the granulite-facies rocks at the northern end of the Serre (Fig. 2) could be of Eocene age, on the basis of K-Ar muscovite data (48 m.y., Borsi and Dubois 1968) from Northern Calabria.

Despite the geochronological work previously done, the age of the granulite-facies metamorphism has not been dated. The present study concentrates on the age of this metamorphism. U-Pb analyses of zircons and monazites and Rb-Sr analyses of whole rocks and minerals were obtained in order to date the pressure-temperature path deduced from petrological investigations (Schenk 1977, 1978). For a better understanding of the temporal relationship between granulite-facies metamorphism and magmatism, zircons from the tonalite and the quartz dioritic gneiss were also analysed. On the other hand, Rb-Sr biotite dates from these rocks should help to clear the postmagmatic cooling and tectonic history of these lithological units. Rb-Sr determinations on mus-

<sup>1</sup> Recalculated using  $\lambda^{87}\text{Rb} = 1.42 \times 10^{-11} \text{ y}^{-1}$

covites and biotites of the phyllonites from the northern most Serre were carried out in order to date the greenschist-facies overprint as well as the earlier metamorphism.

In addition, the radiometric dates can be used to test the relationships suggested above between the Calabrian basement and the granulites of Central Europe of Caledonian age (Jäger and Watznauer 1969; Arnold and Scharbert 1973) or of the Ivrea Zone of the Alps, where the metamorphism ended with a Hercynian event (Köppel 1974).

## 2. Description and Location of the Samples

Samples for U-Pb analyses of zircons and monazites and for the Rb-Sr mineral analyses were collected essentially along a N-S profile through both lithostratigraphic units of the granulite-facies basement of the Serre and also from the quartz dioritic gneiss unit, the tonalite, and the retrograde schists and gneisses. Most of the samples were selected in order to supply zircon, monazite, feldspar and biotite ages of the same rock. Rb-Sr isotopic analyses of whole-rock samples were performed on individual layers of a banded migmatite of the metapelite unit.

### 2.1. Zircon and Monazite Samples

**Granulite KAL-808.** Granulite-pyriclasite unit. New road between Cellia and the chapel S. Croce.

Paragenesis: orthopyroxene-garnet-biotite-potash feldspar-plagioclase-quartz-ilmenite-rutile-pyrrhotite-chalcopyrite-graphite-apatite-zircon-monazite.

Very fine-grained rock.

Rock sample: 19 kg. Zircon: 1.3 g. Monazite: ~ 1 g.

The zircons are homogeneous and typically rounded, ellipsoidal and transparent, colourless or pale pink. They contain very few inclusions and have a very low magnetic susceptibility. Most of the zircons have developed new crystal faces, but their ellipsoidal habit is preserved. Zoning is not revealed by transmitted or reflected light, but a distinct internal heterogeneity becomes visible when studying the cathodoluminescence patterns (Fig. 4a): Nearly all zircons include a relatively small core displaying repeated zoning with euhedral crystal growth zones. The outer, larger zone around the core is fairly homogenous and gives the crystal its oval shape, typical for many zircons of granulite-facies rocks (Grauert and Wagner 1975). The cathodoluminescence of the rim is lighter than that of the core. According to Grauert (1974) these lighter zones reflect lower concentrations of heavy elements like U, Th, and Pb.

The monazite crystals are also ellipsoidal and clear, but yellowish.

**Granulite KAL-85.** Granulite-pyriclasite unit. Some ten meters below the contact to the metapelite unit, at Fosso Umbrita, along the road between Polia and Monterosso.

Paragenesis, rock type, recovery, and description of zircons and monazites as in KAL-808. Rock sample: 10 kg.

**Granulite KAL-147.** Granulite-pyriclasite unit. Small quarry at Zap-terra, 150 m W of the road Polia-Filadelfia.

Paragenesis (but without orthopyroxene), rock type, recovery, and description of zircons and monazites as in KAL-808. Rock sample: 2 kg.

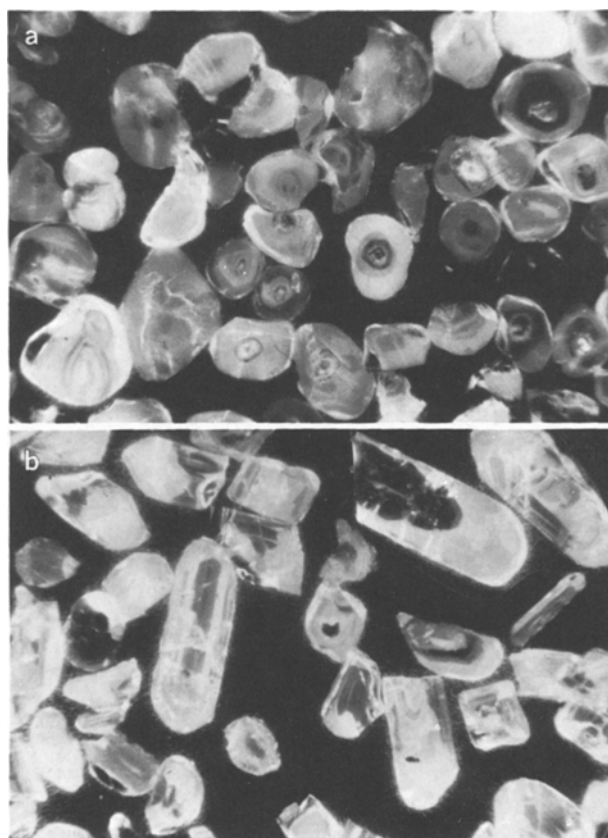


**Fig. 4a and b.** Cathodoluminescence patterns of zircons from two samples of the granulite-facies basement of the NW Serre. Length of the photographs: 0.7 mm. **a** Granulite KAL-808, size-fraction 125–150  $\mu\text{m}$ . Rounded grains consisting of small euhedral zoned cores surrounded by anhedral outer zones. **b** Meta quartz monzogabbro KAL-420, size-fraction > 150  $\mu\text{m}$ . Prismatic euhedral and subeuhedral grains with concentric zoning; in the upper right, a corroded core rich in inclusions

**Pyriclasite KAL-145.** Granulite-pyriclasite unit. Old quarry at Zap-terra along the road between Polia and Filadelfia.

Paragenesis: orthopyroxene-clinopyroxene-biotite-garnet-plagioclase-quartz-pyrrhotite-chalcopyrite-pyrite-ilmenite-apatite-zircon-monazite.

Fine-grained rock with a weak banding of mafic and less mafic layers. Garnet occurs essentially along fine cross fractures.

Rock sample: 48 kg. Zircon: 9 g, of which 60 wt.% are 30–80  $\mu\text{m}$ .

Three zircon populations are distinguishable: (1) Pink, cloudy crystals, mostly short prismatic, (2) Colourless to whitish, cloudy grains, generally ellipsoidal, and (3) Colourless, transparent, ellipsoidal crystals with well-developed crystal faces.

Nearly all zircons have a very low magnetic susceptibility. Only the colourless and whitish zircons in the size-fraction 125–160  $\mu\text{m}$  were enriched by handpicking and analysed.

As for the zircons of KAL-808, zonation was not detected by classical optical methods. But again the cathodoluminescence patterns show large cores with multiple euhedral zones which reflect a former free crystal growth, probably during a magmatic phase. Small, light rims surround the cores incompletely. The zircons are similar to those of KAL-420 (Fig. 4b).

*Pyriclaste KAL-420* (Meta-quartz monzogabbonorite). Metapelite unit. Old quarry, 2 km E of Monterosso.

Paragenesis: orthopyroxene-clinopyroxene-biotite-plagioclase-potash feldspar-apatite-ilmenite-pyrrhotite-zircon.

Homogeneous, medium-grained rock with gneissic texture.

Rock sample: 28 kg. Zircon: 1.8 g, of which more than 80 wt.% are 30–80  $\mu\text{m}$ .

Only the cathodoluminescence makes the zonations visible: Oval shaped, lighter rims surround euhedral, multiple zoned cores, which show in some cases obvious signs of corrosion. Some zircons have irregularly shaped, dark cores, rich in inclusions (Fig. 4b).

The analysed zircons of the size-fraction 100–125  $\mu\text{m}$  are non-magnetic and represent a mixture of two populations: (1) Pink, cloudy, prismatic crystals, and (2) Clear, ellipsoidal grains with numerous, small crystal faces.

The second size-fraction analysed (30–50  $\mu\text{m}$ ) is also non-magnetic and consists of euhedral, clear to pink needles with a length to width ratio of about 4.0.

*Metapelite KAL-170*. Metapelite unit. Stream, 1 km S of Capistrano.

Paragenesis: garnet-cordierite-sillimanite-biotite-potash feldspar-plagioclase-graphite-ilmenite-rutile-pyrrhotite-chalcopryrite-apatite-zircon-monazite.

Coarse-grained rock with fractured garnets which have been rotated after crystallization.

Rock sample: 11 kg. Zircon: 8 mg. Monazite: 2–3 g. Similar quantity ratios between zircon and monazite occur in other high-grade metamorphic pelites from the Moldanubicum (Grauert et al. 1974).

The zircons are in all respects similar to those from the granulite sample KAL-808. The most abundant crystals are small (< 30  $\mu\text{m}$ ), clear and ellipsoidal. The zircon sample was not divided into different size-fractions because of low recovery.

The most abundant monazites are smaller than 50  $\mu\text{m}$ . These crystals are clear, yellowish green, and ellipsoidal.

*Metapelites KAL-90, -168, -489, -879*. All from the metapelite unit.

Paragenesis similar to that of KAL-170, but with  $\pm$  quartz  $\pm$  plagioclase  $\pm$  potash feldspar.

Because only monazites had to be separated, small samples of 0.5 to 6 kg were crushed.

KAL-90: 800 m NE of Monterosso, 50 m E of the road Monterosso-Polia. KAL-168: 1.3 km S of Capistrano, small quarry 50 m E of the road Capistrano-S. Nicola. KAL-489: Torrente Falla, 500 m N of S. Nicola. KAL-879: 150 m S of the cemetery of S. Nicola.

*Quartz Dioritic Gneiss KAL-887*. Stream, 100 m NW of Vallelonga.

Paragenesis: cummingtonite-green hornblende-biotite-plagioclase-quartz-apatite-clinozoisite-carbonate-opaque ore-zircon.

Coarse-grained gneiss with blastomylonitic texture.

Rock sample: 1.7 kg. Zircon: 0.5 g.

Homogeneous zircon population of clear euhedral needles of pink color. A regular, concentric zoning is visible using the cathodoluminescence method. In some of the zircons, irregularly shaped (corroded?) cores are present.

*Tonalite KAL-730*. 1 km E of Cardinale, on the new road to Satriano.

Paragenesis: plagioclase-quartz-biotite-apatite-carbonate-clinozoisite-sphene-zircon.

Rock sample: 3 kg. Zircon: 0.25 g.

The zircons are in all respects similar to those of sample KAL-887. Their regular idiomorphic zoning may indicate a magmatic crystallization.

## 2.2. Rb-Sr Whole-Rock Samples

A large sample of a migmatitic,  $\text{Al}_2\text{O}_3$ -rich paragneiss (KAL-168) was collected from the metapelite unit about 1 km S of Capistrano (Fig. 2). The sample represents a 45 cm thick portion of a banded migmatitic gneiss and consists mainly of melanosomes with two leucosomes and a calc-silicate layer. A 5 cm thick plate was cut perpendicular to the layers and divided in 15 petrographically homogeneous samples, 2–5 cm thick, from which 10 were chosen for analysis on the basis of their Rb/Sr ratios. The analysed samples are:

*A*: Quartz-plagioclase-potash feldspar leucosome rich in potash feldspar.

*N*: Quartz-plagioclase-potash feldspar leucosome poor in potash feldspar.

*F*: Sample rich in leucosome which also contains pieces of melanosome.

*C, G, I, L, M*: Melanosomes with garnet-biotite-cordierite-sillimanite-plagioclase  $\pm$  quartz  $\pm$  potash feldspar.

*K*: Calc-silicate consisting of anorthite rich plagioclase, quartz, garnet and biotite.

*KL*: Border zone of layer K which adjoins layer L, enriched in biotite.

## 2.3. Samples for the Rb-Sr Mineral Analyses

The rock samples chosen for Rb-Sr mineral dating were of very small size (30–50 g) in order to get mineral concentrates as homogeneous as possible, chemically and isotopically. If possible, analyses of biotite, potash feldspar, plagioclase, apatite, and whole-rock were performed on the same sample. Muscovite is absent from the granulite-facies rocks and also from the quartz dioritic gneisses and the tonalite but could be dated in one aplite in the upper part of the metapelite unit and in the retrograde schists and gneisses north of the Curinga-Girifalco line (Fig. 2).

Most samples selected for Rb-Sr mineral dating are the same as for zircon and monazite analyses (2.1) and, therefore, will not be listed again.

*Granulite KAL-808*. Granulite-pyriclaste unit. New road between Cellia (Polia) and the chapel S. Croce.

Paragenesis: garnet-biotite-potash feldspar-plagioclase-quartz-ilmenite-rutile-pyrrhotite-chalcopryrite-graphite-apatite-zircon-monazite.

Homogeneous, fine-grained rock.

*Metapelite KAL-370*. Metapelite unit. Fosso Ferraro, 150 m SE of the road Polia-Monterosso.

Paragenesis: garnet-biotite-sillimanite-potash feldspar-quartz-graphite-ilmenite-rutile-pyrrhotite-chalcopryrite-apatite-zircon-monazite.

Fine-grained rock with gneissic texture.

*Garnet-Biotite Gneiss KAL-657*. Metapelite unit. Fosso Cataratti, 1 km SE of the road Polia-Monterosso.

Paragenesis: garnet-biotite-potash feldspar-plagioclase-quartz-apatite-ilmenite-pyrrhotite-chalcopryrite-zircon.

Fine-grained rock with gneissic texture. Potash feldspar (~ 4 Vol.%) is not homogeneously distributed, but enriched in patches.

*Aplite KAL-491*. Metapelite unit. Torrente Falla, 400 m NE of S. Nicola.

Paragenesis: biotite-muscovite-potash feldspar-plagioclase-quartz-apatite-zircon.

Fine-grained, homogeneous rock, with a schistose texture.

*Meta-Quartz Monzogabbronite KAL-94.* Same intrusive body as zircon sample KAL-420 M, metapelite unit, along the road between Monterosso and Capistrano.

Paragenesis: orthopyroxene-clinopyroxene-biotite-plagioclase-potash feldspar-apatite-ilmenite-pyrrhotite-zircon.

Homogeneous, medium-grained rock with gneissic texture.

*Phyllonitic Gneiss KAL-51.* Unit of the retrograde schists and gneisses, north of the Curinga-Girifalco line. Road bridge across the Fiume Pesipe, 1.5 km W of Cortale.

Paragenesis: potash feldspar-plagioclase-quartz-muscovite-garnet-clinozoisite-apatite-zircon-opaque ore.

Muscovite is present as big, deformed porphyroblasts, but essentially as fine crystalline matrix along shear planes.

*Phyllonitic Mica Schist KAL-42.* Unit of the retrograde schists and gneisses, north of the Curinga-Girifalco line. Road, 1.5 km ENE of Curinga.

Paragenesis: garnet-biotite-muscovite-clinozoisite quartz-plagioclase-apatite-zircon and/or monazite-opaque ores.

### 3. Analytical Procedures

#### 3.1. U-Pb Isotopic Analyses

Zircon and monazite concentrates, obtained by using a Wilfley table and heavy liquids, were washed in hot 6N HCl followed by hot 6N HNO<sub>3</sub>. Grain size fractions (nylon sieves) were further divided according to their magnetic susceptibility using a Frantz electro-magnetic separator. Only zircons of low magnetic susceptibility (non-magnetic at 1.6 A and 0.5 degree lateral tilt) were analysed. The last cleaning of the zircon and monazite fractions (8 to 45 mg) was performed by hand-picking.

For extraction of U and Pb, the chemical procedure developed by Krogh (1973) was used. Aliquots of the dissolved samples were spiked with a combined <sup>208</sup>Pb-<sup>235</sup>U tracer.

Isotopic analyses were performed on a Teledyne (SS-1290) solid source mass spectrometer equipped with a peakhopping system, a Cary 401 vibrating reed amplifier and an on-line computer. Pb was measured using a Re single filament and the silica gelphosphoric acid load technique (Cameron et al. 1969). U was measured on a Re single filament with a mixture of TaO<sub>2</sub> and Ta as activator.

The isotopic composition of common Pb used for corrections are: <sup>206</sup>Pb/<sup>204</sup>Pb = 18.27, <sup>207</sup>Pb/<sup>204</sup>Pb = 15.59 and <sup>208</sup>Pb/<sup>204</sup>Pb = 38.17. The following constants were used:  $\lambda^{238}\text{U} = 1.5513 \times 10^{-10} \text{y}^{-1}$ ,  $\lambda^{235}\text{U} = 9.8485 \times 10^{-10} \text{y}^{-1}$  and  $^{238}\text{U}/^{235}\text{U} = 137.88$ . The assigned analytical uncertainties are: <sup>206</sup>Pb/<sup>238</sup>U:  $\pm 1.0\%$ , <sup>207</sup>Pb/<sup>206</sup>Pb:  $\pm 0.5\%$ , <sup>207</sup>Pb/<sup>235</sup>U:  $\pm 1.0\%$ . Regression calculations were performed by the least squares method of York (1969).

#### 3.2. Rb-Sr Isotopic Analyses

Pulverization of whole-rocks and mineral separation were performed using standard techniques. Sample splits of about 100 mg were dissolved in Teflon beakers with HF+HNO<sub>3</sub>(3:1), A combined <sup>87</sup>Rb-<sup>84</sup>Sr spike was used. Rb and Sr were separated by ion exchange techniques.

Rb was loaded as chloride on the side filament (Ta) of a triple filament source, Sr as a phosphate on a single Ta filament. The mass spectrometer used was the same as that used for U and Pb analyses.

Regression calculations were performed by the least-squares method of York (1969) using  $\lambda^{87}\text{Rb} = 1.42 \times 10^{-11} \text{y}^{-1}$  (Steiger and

Jäger 1977). Age and initial ratio errors are given at the 95% (2 $\sigma$ ) confidence level, assuming analytical errors on <sup>87</sup>Rb/<sup>86</sup>Sr of 0.5% and on <sup>87</sup>Sr/<sup>86</sup>Sr to be not greater than the internal uncertainty of the measurements.

### 4. Discussion of the Analytical Results

#### 4.1. U-Pb Analyses of Zircons and Monazites

The results of the U and Pb analyses are listed in Table 1 and plotted on a concordia diagram (Wetherhill 1956) in Fig. 5. Four groups of data points can be distinguished in the diagram:

1. The first group lies on a chord which intersects the concordia at  $296 \pm 2$  m.y. and at  $1,890 \pm 60$  m.y. The data points correspond to four grain size fractions of the granulite zircons KAL-808, the whole zircon fraction from the restitic metapelite KAL-170, and the 100–125  $\mu\text{m}$  fraction of the metamorphosed quartz monzogabbronite KAL-420. The 30–50  $\mu\text{m}$  fraction of KAL-420 was not used for calculation of the regression line because the analytical results are somewhat uncertain, as they show a high common lead content (see the low <sup>206</sup>Pb/<sup>204</sup>Pb ratio in Table 1).

2. The second group comprises concordant monazites and zircons. Six monazites from granulite-facies rocks lay concordant between 296 and 289 m.y. One monazite (KAL-90), coming from the lowest part of the metapelite unit, indicates a somewhat younger concordant age of 283 m.y. The two zircons of the tonalite KAL-730 are also concordant at  $295 \pm 2$  m.y.

3. The zircon fraction of a pyriclasite from the granulite-pyriclasite unit (KAL-145) shows a discordance quite different from that of all other zircons of the granulite-facies basement (see group 1).

4. Two zircon fractions of the blastomylonitic quartz dioritic gneiss KAL-887 constitute the fourth group, lying near a line which intersects the concordia at the origin and at about 290 m.y.

The pattern of the first group may be explained by one or both of two simple models: (a) All analysed zircons crystallized at 1,900 m.y. Through a secondary event at 296 m.y., they lost radiogenic lead or gained uranium (episodic model; Wetherhill 1956). (b) The analysed zircon fraction are mixtures of 296 and 1,900 m.y. old concordant zircons. According to this model, the growth of the 296 m.y. old zircons was caused by a metamorphic event which ended in late Hercynian time. The same age is also indicated by the concordant monazites.

The zircons of KAL-808 and KAL-170 have similar appearance and habit and both display a late stage crystal growth which in other granulite terranes has been interpreted as having occurred during granulite-

**Table 1.** Analytical data of zircons and monazites

	Sieve fraction ( $\mu\text{m}$ )	Concentrations		Observed atomic ratios			Atomic ratios			Apparent ages (m.y.)			
		U (ppm)	Pb <sub>rad</sub> (ppm)	$\frac{^{208}\text{Pb}}{^{206}\text{Pb}}$	$\frac{^{207}\text{Pb}}{^{206}\text{Pb}}$	$\frac{^{206}\text{Pb}}{^{204}\text{Pb}}$	$\frac{^{206}\text{Pb}}{^{238}\text{U}}$	$\frac{^{207}\text{Pb}}{^{235}\text{U}}$	$\frac{^{207}\text{Pb}}{^{206}\text{Pb}}$	$\frac{^{206}\text{Pb}}{^{238}\text{U}}$	$\frac{^{207}\text{Pb}}{^{235}\text{U}}$	$\frac{^{207}\text{Pb}}{^{206}\text{Pb}}$	
<u>Zircons</u>													
KAL-808	Granulite	30–50	428	23.8	0.09937	0.06375	17,100	0.05563	0.4825	0.06291	349	400	706
		50–75	425	23.8	0.09845	0.06494	16,300	0.05620	0.4965	0.06407	353	409	744
		100–125	761	42.6	0.10323	0.06513	38,250	0.05576	0.4979	0.06475	350	410	766
		125–150	463	25.6	0.12115	0.06598	4,004	0.05470	0.4706	0.06239	289	392	687
KAL-170	Aluminous paragneiss	all sieve fractions	439	19.7	0.03986	0.05651	6,030	0.04800	0.3581	0.05410	302	311	376
KAL-420	Meta-quartz monzogabbronorite	30–50	220	12.4	0.24380	0.75344	632	0.04817	0.3466	0.05218	303	302	294
		100–125	211	11.1	0.19944	0.06630	1,055	0.04727	0.3417	0.05242	298	298	304
KAL-145	Pyriclastite	125–160	446	24.1	0.15113	0.05907	2,490	0.05157	0.3783	0.05320	324	326	337
KAL-730	Tonalite	30–50	410	20.7	0.19483	0.05631	3,670	0.04653	0.3356	0.05232	293	294	299
		> 100	448	21.9	0.14855	0.05623	3,600	0.04686	0.3371	0.05216	295	295	293
KAL-887	Quartz dioritic gneiss	50–80	1,255	38.2	0.17441	0.05374	10,410	0.02877	0.2076	0.05234	183	192	300
		> 125	852	41.6	0.30051	0.05347	9,960	0.04179	0.2996	0.05220	264	266	286
<u>Monazites</u>													
KAL-147	Granulite		2,266	885.6	8.5353	0.05441	6,950	0.04690	0.3383	0.05230	296	296	298
KAL-85	Granulite		906	443.1	11.0450	0.05509	4,870	0.04644	0.3335	0.05208	292	292	290
KAL-90	Aluminous paragneisses		2,204	578.8	5.6870	0.05475	5,310	0.04480	0.3212	0.05199	283	283	286
KAL-170			2,140	639.5	6.4646	0.05321	12,620	0.04582	0.3289	0.05206	289	289	290
KAL-168			2,555	717.6	5.8627	0.05363	11,770	0.04680	0.3380	0.05238	295	296	302
KAL-489			2,136	587.7	5.8476	0.05362	8,910	0.04593	0.3291	0.05197	290	290	285
KAL-879			739	596.1	18.9018	0.05870	2,240	0.04620	0.3322	0.05216	291	291	293

facies metamorphism (Grauert and Wagner 1975; Köppel 1974; Pidgeon and Aftalion 1972). Therefore, in accordance with the observed zonation (Fig. 4a), it seems reasonable to attribute the discordant pattern of the zircons from KAL-808 and KAL-170 essentially to crystal growth and overgrowth in addition to possible lead loss during the Hercynian granulite-facies metamorphism.

From the concordant positions of both size fractions of the metamorphosed quartz monzogabbronorite KAL-420, which represent the smallest and the largest grains, it may be deduced that the intrusion of the sill into the lower crust coincided nearly with the end of the metamorphism. The inherited dark cores observed in some grains (see 2.1 and Fig. 4b) obviously lost their older radiogenic lead during the magmatic phase of the rock.

The concordant monazites (second data group) fall nearly together with the lower intersection point of the concordia with the discordia drawn through the zircons of the granulite-facies rocks (first data

group). This indicates that in the whole section through the lower crust, which is about 7 km thick, monazite became a closed system in respect to U and Pb at the same time as, or shortly after, zircon. The slightly younger age of the monazite from KAL-90 ( $283 \pm 3$  m.y.) possibly indicates that at the base of the metapelite unit the monazites lost radiogenic lead also after the metamorphic event dated above.

The concordant zircons of the non-metamorphic tonalite KAL-730 imply the same age ( $295 \pm 2$  m.y.) for the intrusion of the big tonalite body of the Serre as that determined for the end of the metamorphism.

The discordant zircon fraction of the pyriclastite KAL-145 (third group of data points) seems to reflect quite a different history than the zircons discussed above. Assuming a two stage model for their genesis, as suggested by the cathodoluminescence pattern, the first stage may correspond to the magmatic crystallization and the second to the granulite-facies metamorphism. As the metamorphism has been dated at 296 m.y., the age of the magmatic crystallization may

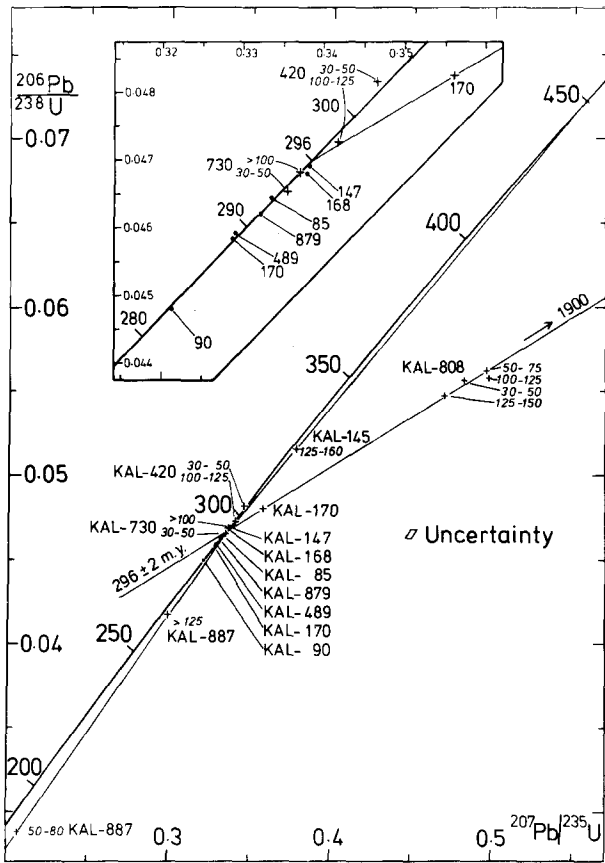


Fig. 5. Concordia diagram showing the data points of zircons and monazites of 12 samples from the NW Serre. *Italic numbers*: size-fractions in  $\mu\text{m}$ ; *Points*: monazites; *crosses*: zircons

be inferred by constructing a discordia going through the 296 m.y. point on the concordia and through the data point of the zircon from KAL-145; the upper intersection between this discordia and the concordia, lying at about 450 m.y., could represent the age of the magmatic crystallization of the pyriclaste KAL-145.

The two zircon fractions of KAL-887 (fourth data group) have similar  $^{207}\text{Pb}/^{206}\text{Pb}$  ages of 300 and 286 m.y. respectively, which coincide roughly with the event indicated by the first and the second groups of analyses. Therefore it is probable that these  $^{207}\text{Pb}/^{206}\text{Pb}$  ages reflect the time of zircon crystallization. The discordant position of the data points, which fall on a line that intersects the concordia at about 290 m.y. and passes through the origin, can be explained by recent or geologically young Pb-loss or U-gain.

#### 4.2. Rb-Sr Analyses of Whole-Rocks

The analytical results of Rb-Sr whole-rock analyses of small slabs of the banded migmatite KAL-168 are listed in Table 2 and plotted in Fig. 6. In the Rb-Sr evolution diagram, the points do not lie on an isochron. It may thus be postulated that conditions during migmatization did not allow homogenization of the Sr isotopes throughout the large sample KAL-168. Alternatively, a later thermal event, after the peak of metamorphism or migmatization, allowed some migration of Rb and Sr among the layers but did not homogenize the Sr isotopes.

Interestingly, the points of the two leucosomes A and N lie on a line with a slope corresponding to an age of about 295 m.y., an age also indicated by the U-Pb analyses. This may result from isotopic equilibration among the anatectic layers during metamorphism, although the intercalated melanosomes did not equilibrate. Alternatively, a later thermal event may have allowed limited isotopic exchange between the melanosomes but not between the biotite-free leucosomes which preserved their isotopic composition.

#### 4.3. Rb-Sr Mineral Analyses

Biotite ages were determined from ten samples along the profile through the granulite-facies basement. Muscovite was found in only one post-metamorphic aplite. In order to get more information about the cooling history of the basement, and in absence of muscovite in granulite-facies rocks, plagioclase, potash feldspar (orthoclase), and apatite were analysed

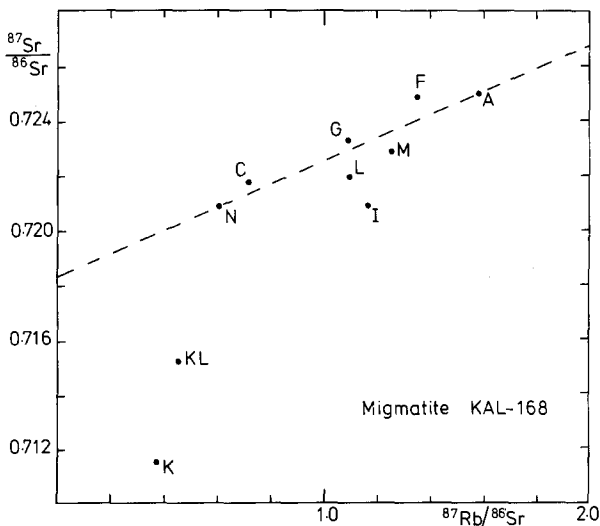


Fig. 6. Rb-Sr whole-rock evolution diagram for bands of a migmatite of the metapelite unit, NW Serre. The line through the leucosome points A and N is drawn for reference. The slope corresponds to an age of 295 m.y.



**Table 2.** Rb-Sr analytical data of whole-rock and minerals

		Rb (ppm)	Sr (ppm)	$^{87}\text{Rb}/^{86}\text{Sr}$	$^{87}\text{Sr}/^{86}\text{Sr}$	Initial ratio	Age (m.y.)
KAL-42	Muscovite	532.0	75.2	20.7	$0.79609 \pm 1$	} 0.7170 $\pm 4$	268 $\pm 4$
	Whole-rock	623.3	184.4	9.83	$0.75457 \pm 2$		
	Biotite	1,667.7	17.7	279	$0.91987 \pm 7$		
KAL-51	Whole-rock	194.5	69.9	8.09	$0.75183 \pm 8$	} 0.7272 $\pm 2$	214 $\pm 2$
	Muscovite	604.6	26.8	66.7	$0.93003 \pm 29$		
KAL-147	Whole-rock	97.6	167.2	1.69	$0.72349 \pm 7$	} 0.72107 $\pm 5$	108 $\pm 1$
	Biotite	585.7	5.0	356	$1.26887 \pm 10$		
	Apatite	0.5	128.8	0.0122	$0.72253 \pm 14$		
	Plagioclase	19.1	176.9	0.313	$0.72091 \pm 6$		
	K-feldspar	230.4	366.7	1.82	$0.72405 \pm 4$		
KAL-808	Whole-rock	89.6	154.6	1.68	$0.72140 \pm 9$	} 0.71867 $\pm 9$	114 $\pm 1$
	Biotite	647.1	9.7	199	$1.04110 \pm 9$		
	Apatite	1.8	100.6	0.0511	$0.71906 \pm 4$		
	Plagioclase	34.6	141.9	0.708	$0.71980 \pm 9$		
	K-feldspar	265.0	309.2	2.47	$0.72341 \pm 5$		
KAL-85	Whole-rock	72.1	167.9	1.25	$0.71967 \pm 5$	} 0.71769 $\pm 5$	112 $\pm 1$
	Biotite	580.7	8.8	198	$1.03171 \pm 7$		
	Apatite	1.4	162.4	0.0243	$0.71822 \pm 9$		
	Plagioclase	22.1	180.9	0.354	$0.71815 \pm 4$		
	K-feldspar	210.4	453.6	1.35	$0.72014 \pm 6$		
KAL-370	Whole-rock	87.0	110.6	2.28	$0.73078 \pm 5$	} 0.7279 $\pm 2$	88 $\pm 1$
	Biotite	731.7	8.6	254	$1.04567 \pm 25$		
KAL-657	Whole-rock	79.4	314.4	0.732	$0.71645 \pm 29$	} 0.7154 $\pm 3$	101 $\pm 1$
	Biotite	325.3	8.4	115	$0.88049 \pm 2$		
	Apatite	1.8	281.9	0.0184	$0.71650 \pm 15$		
	Plagioclase	12.3	408.6	0.0872	$0.71532 \pm 14$		
	K-feldspar	122.9	760.4	0.468	$0.71552 \pm 12$		
	K-feldspar(repeated)	123.2	760.5	0.469	$0.71542 \pm 9$		
KAL-94	Whole-rock	77.6	199.0	1.13	$0.71507 \pm 7$	} 0.71290 $\pm 6$	135 $\pm 1$
	Biotite	588.1	5.0	367	$1.41704 \pm 10$		
	Apatite	1.5	114.3	0.0388	$0.71554 \pm 6$		
	Plagioclase	4.6	299.4	0.0446	$0.71239 \pm 6$		
	K-feldspar	273.8	393.7	2.02	$0.71734 \pm 6$		
KAL-170	Whole-rock	127.0	126.3	2.92	$0.73046 \pm 14$	} 0.7250 $\pm 1$	132 $\pm 1$
	Biotite	503.7	4.6	325	$1.35316 \pm 33$		
KAL-168	Whole-rock	61.0	211.1	0.839	$0.72261 \pm 2$	} 0.72101 $\pm 7$	134 $\pm 1$
	Biotite	496.4	6.3	238	$1.17526 \pm 11$		
	Plagioclase	6.7	488.7	0.0396	$0.72096 \pm 4$		
	K-feldspar	191.0	656.6	0.844	$0.72131 \pm 3$		
KAL-491	Muscovite	154.3	140.4	3.18	$0.71298 \pm 4$	} 0.7038 $\pm 1$	203 $\pm 4$
	Plagioclase	8.3	648.6	0.0369	$0.70390 \pm 16$		
	Biotite	371.4	5.5	203	$1.03193 \pm 5$		
KAL-879	Plagioclase	1.3	613.5	0.0061	$0.71274 \pm 4$	} 0.71273 $\pm 4$	134 $\pm 1$
	Biotite	309.4	8.2	112	$0.92657 \pm 5$		
KAL-887	Plagioclase	0.8	239.3	0.0095	$0.71136 \pm 8$	} 0.71135 $\pm 7$	85 $\pm 1$
	Biotite	272.3	18.1	43.9	$0.76403 \pm 6$		
KAL-730	Whole-rock	81.9	285.1	0.832	$0.71346 \pm 8$	} 0.7119 $\pm 1$	133 $\pm 1$
	Biotite	321.7	1.3	803	$2.22801 \pm 40$		
KAL-168	A Leucosome	211.6	388.6	1.58	$0.72503 \pm 10$	}	
	C Melanosome	55.4	223.1	0.721	$0.72178 \pm 7$		
	F Melanosome + leucosome	174.0	373.3	1.35	$0.72485 \pm 14$		
	G Melanosome	87.1	229.9	1.10	$0.72329 \pm 9$		
	I Melanosome	102.2	253.7	1.17	$0.72098 \pm 13$		
	K Calc-silicate	53.6	421.6	0.368	$0.71152 \pm 28$		
	KL Melanosome	56.4	361.4	0.452	$0.71525 \pm 56$		
	L Melanosome	96.8	256.5	1.09	$0.72202 \pm 8$		
	M Melanosome	63.7	147.6	1.25	$0.72292 \pm 16$		
	N Leucosome	41.6	199.3	0.605	$0.72092 \pm 9$		

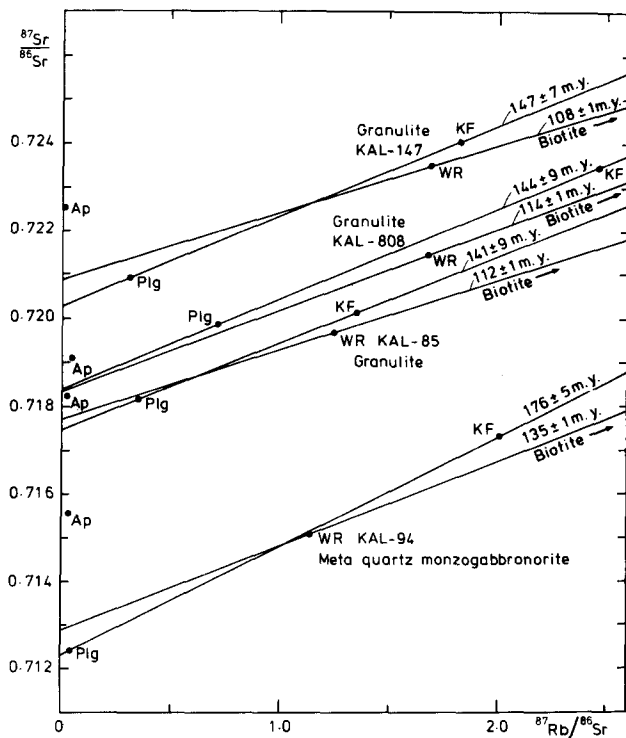


Fig. 7. Rb-Sr evolution diagram for minerals of four small rock samples from the lower crust section in the NW Serre. Abbreviations: *WR* whole-rock, *KF* potash feldspar, *Plg* plagioclase, *Ap* apatite

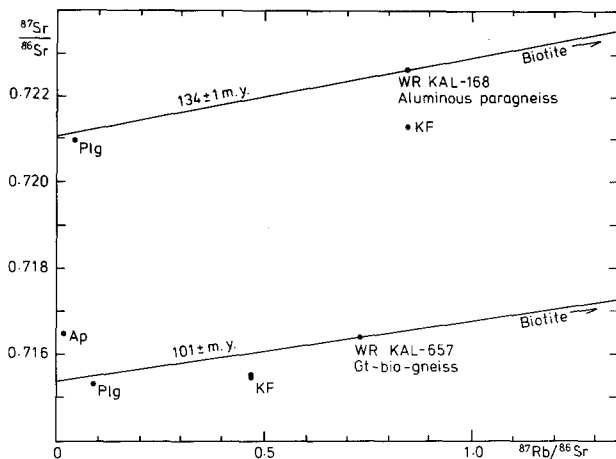


Fig. 8. Rb-Sr evolution diagram for minerals of two small rock samples from the metapelite unit, NW Serre. Abbreviations as in Fig. 7

from six samples, in addition to biotite and whole-rock. The analytical results are given in Table 2, some of which are plotted in Figs. 7 and 8.

In all analysed samples, the minerals of a rock do not lie on an isochron, which means that they did not close their Rb-Sr systems at the same time.

The results can be divided in two groups:

(1) The first group is represented by four rocks, three granulites and the metamorphosed quartz monzogabbonorite. As shown in Fig. 7, the biotites fall systematically below and the apatites above the lines drawn through the plagioclases and the potash feldspars. The whole-rock analyses have to lie somewhere in the field determined by the four minerals, which is verified for three of the analysed rocks, but not in the case of KAL-808, in which the whole-rock sample does not seem to be representative of the rock. The biotite ages from the three samples of the granulite-pyriclasite unit are very similar (between 108 and 114 m.y.), the plagioclase-potash feldspar ages from the same rocks identical within analytical uncertainty (141–147 m.y.). Moreover, the higher feldspar ages ( $176 \pm 5$  m.y.) from sample KAL-94 of the metapelite unit is accompanied by a correspondingly higher biotite age ( $135 \pm 1$  m.y.) from the same sample. The systematic isotopic pattern in the minerals of the four rocks is interpreted as due to different Rb-Sr closing temperatures of the minerals: higher closing temperatures for plagioclase and orthoclase than for biotite and apatite. Similarly, the muscovite data of  $203 \pm 4$  m.y. from the metapelite unit points to a higher closing temperature for muscovite than for feldspar.

(2) The data pattern of the metapelitic gneisses KAL-168 and KAL-657 are characterized by low  $^{87}\text{Sr}/^{86}\text{Sr}$  ratios of their potash feldspars in relation to the other minerals (Fig. 8). These gneisses are petrographically different from the rocks of the first group: the granulites and the metamorphosed quartz monzogabbonorite of the first group have granoblastic textures and all their minerals are distributed homogeneously, so that a grain by grain isotopic exchange between the minerals probably took place. Contrary to the above, potash feldspar in the metapelitic gneisses is enriched in small patches and lenses, which may be anatectic material and, therefore, not in isotopic equilibrium with the rest of the rock. This may explain the low  $^{87}\text{Sr}/^{86}\text{Sr}$  ratios of the potash feldspars from the two analysed metapelitic gneisses.

Comparing the apparent mica ages from the different lithological units of the Serre, the following facts are worthy of comment (Fig. 9): (a) In the granulite-pyriclasite unit, the biotite ages of 108 and 114 m.y. are younger than those in the metapelite unit, where ages of 132–135 m.y. are predominant, and also younger than that of the tonalite ( $133 \pm 1$  m.y.). (b) Some biotite ages do not fit this picture: towards the base of the metapelite unit, these ages become younger, from  $135 \pm 1$  m.y. to  $101 \pm 1$  m.y. and  $88 \pm 1$  m.y. Near the top of the metapelite unit, the biotite of a postmetamorphic aplite

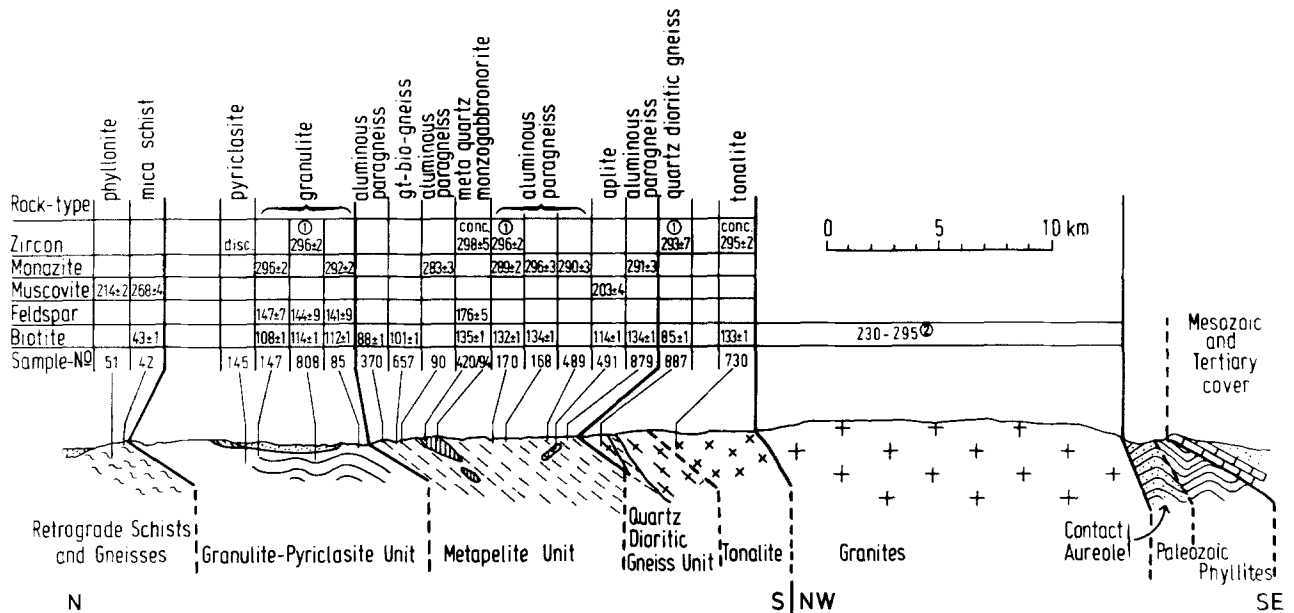


Fig. 9. Distribution of U-Pb and Rb-Sr mineral dates along the studied section through the Serre. 1: discordant zircons; age indicated by an intersection of the discordia with the concordia. 2: biotite model ages from Borsi et al. (1976), recalculated using  $\lambda^{87}\text{Rb} = 1.42 \times 10^{-11} \text{y}^{-1}$

has also a younger age of 114 m.y., and, further, the biotite from the blastomylonitic quartz dioritic gneiss, situated between the granulite-facies basement and the tonalite, has an age of  $85 \pm 1$  m.y. (c) The biotite from the phyllonitic mica schist (KAL-42) is, with an age of  $43 \pm 1$  m.y., clearly younger than the biotites from the granulite-facies rocks. Interpreting the muscovite age ( $268 \pm 4$  m.y.) from the same rock, one must take into account the possibility of an incomplete separation of the large, texturally old, muscovites from the small, younger white micas. In case of the sample KAL-51, the unsuccessful separation from the texturally younger white micas result in the meaningless mixed muscovite age of  $214 \pm 2$  m.y.

## 5. Geological Conclusions

### 5.1. Interpretation of the Results

The oldest material analysed from the granulite-facies rocks of the Serre are zircons. They contain inherited components which are derived from a much older source. The upper intersection age of about 1,900 m.y. may represent the age of the source rock or may only be a mixed age. The age of about 295 m.y., indicated by zircons and concordant monazites, is interpreted as the minimum age of the granulite-facies metamorphism in Southern Calabria. This thermal event at 295 m.y. resulted in crystal growth of zircon

and monazite in the granulite-facies rocks of the Serre.

The magmatic crystallization of the pre- to synmetamorphic basic rocks (now pyriclasites) of the granulite-pyriclasite unit may be as old as 450 m.y., assuming a two stage genetic model for the zircons. As the basic rocks are interlayered with light-coloured granulites of sedimentary origin, the age of 450 m.y. should then represent the minimum age of the sedimentation, i.e. the formation of the former lower crust.

The age of  $298 \pm 5$  m.y. for the concordant zircons of a metamorphosed quartz monzogabbronorite coincides closely with the end of the granulite-facies metamorphism. If the euhedral zircon needles are of magmatic origin, as implied by the similarity in habit and zonation to magmatic zircons, it is most probable that the intrusion of the 250 m thick quartz monzogabbronorite sill into the lower crust occurred during the late stage of the granulite-facies metamorphism.

At about the same time as the intrusion of the 'synmetamorphic' quartz monzogabbronorite into the lower crust, the big 'postmetamorphic' tonalite body intruded at higher crustal levels, as indicated by its concordant zircons at  $295 \pm 2$  m.y. The zircons of the quartz dioritic gneisses also point to a magmatic crystallization in late Hercynian times. The huge mass of granites and granodiorites of the Serre also seems to be of the same age, as inferred from the biotite model ages of Borsi et al. (1976) (Fig. 9).

Considering the metamorphism prior to the phyllonitization in the retrograde schists and gneisses lying below the lower crust unit, its Hercynian age is indicated by a muscovite date of  $268 \pm 4$  m.y. from a mica schist. As this analytical result may have been influenced by a younger muscovite generation in the same rock, the end of the metamorphism in the unit of the retrograde schists and gneisses could have been in fact at about 295 m.y., i.e. the same age as in the granulite-facies unit. The biotite date of  $43 \pm 1$  m.y. from the same mica schist is in good agreement with a K-Ar age of 48 m.y. from a deeper tectonic unit in Northern Calabria (Borsi and Dubois 1968). In analogy to the interpretation of Borsi and Dubois, this date may represent the age of the Eocene greenschist-facies metamorphism and phyllonitization in the retrograde schists and gneisses.

The apparent ages of biotite, feldspar, and muscovite from the granulite-facies unit, the tonalite, and the quartz dioritic gneiss are clearly younger than metamorphism and magmatism. The muscovite is oldest, feldspars are intermediate, and biotites are the youngest (Fig. 9).

This sequence presumably reflects the different closing temperatures of the three minerals which are estimated to span an interval of about  $200^\circ\text{C}$ . Moreover, comparison of mineral ages from samples of the metapelite unit and of the granulite-pyriclasite unit shows that the granulites lying deeper in the lithostratigraphic sequence generally yield the younger ages. Thus the cooling from the temperature of the granulite-facies metamorphism to the biotite closing temperature required about 185 m.y. in the lower part of the succession, but only about 160 m.y. in the upper part. This difference may be explained by a model in which cooling started in the lower part with higher metamorphic temperatures. Assuming that the Rb-Sr systems behaved similarly in the feldspars and in the biotites from all the analysed samples, one can draw the following conclusions. During the cooling period of the granulite-facies basement between about 295 and 110 m.y., the lower part of the sequence was hotter, and, therefore, probably buried more deeply than the upper part. Under these assumptions a tentative cooling path for the lower crust section is drawn in Fig. 10.

It is not possible to give an unequivocal explanation for some biotite dates from the upper part of the section, which give younger ages (85, 88 and 101 m.y., Fig. 9). Interestingly, these deviations seem to be related to the presence of tectonic zones still active during the postmetamorphic uplift: (1) Considering its blastomylonitic texture and its geological position between the lower crust unit and the tonalite, the quartz dioritic gneiss unit could have acted as

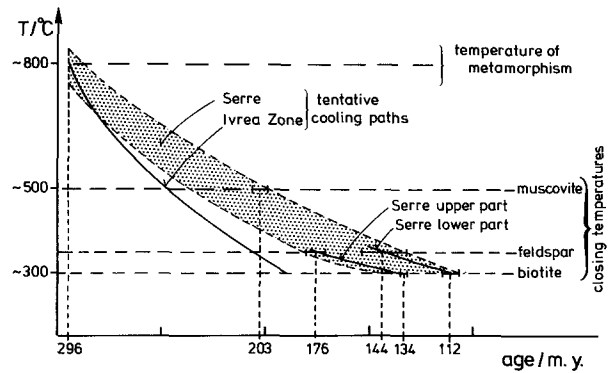


Fig. 10. Tentative cooling path for the granulite-facies sequence of the NW Serre, as deduced from radiometric ages of zircons, monazites, feldspars, and biotites. For comparison, a cooling curve for the Ivrea Zone has been constructed using data from zircon (Köppel 1974) and biotite (Graeser and Hunziker 1968)

a shear zone during the uplift. Not only its biotite is rejuvenated but also its zircons display geologically young or recent lead loss. (2) Along the boundary between the granulite-pyriclasite unit, tectonic movements during the uplift are documented by mylonitic and pseudotachylitic zones which are locally up to ten meters thick. Also the monazite from the zone of increasing biotite rejuvenation gives a somewhat younger age ( $283 \pm 3$  m.y., instead of 289–296 m.y.). (3) The aplite from the upper part of the metapelite unit obviously intruded after the granulite-facies metamorphism, as indicated by the paragenesis muscovite + quartz, which was unstable in the surrounding granulite-facies rocks. The clear schistosity of this rock is an unequivocal sign of late tectonic shearing. Thus all deviations towards younger biotite ages may be explained by a tectonic influence on the closing of biotite in respect to Rb and Sr. In all the other samples the biotites probably closed their Rb-Sr systems under more or less static conditions.

The very slow cooling of the basement of the Serre could explain the scatter of the Rb-Sr whole-rock analyses of the migmatite bands (Fig. 6): Because of the long duration of cooling, the biotite-bearing melanosomes could exchange Sr-isotopes to some extent, while the biotite-free leucosomes perhaps preserved their original isotope distribution and thus indicate the time of the highest metamorphic conditions at about 295 m.y.

The age data presented above correlate well with the *P-T* history of the lower crustal rocks deduced from petrological studies (Schenk 1977, 1978) and with the geodynamic evolution of Southern Calabria inferred from observations on erosion and sedimentation (Görlner and Giese 1978): The isothermal pressure decrease of approximately 1.5 to 2 kb that followed the peak of granulite-facies metamorphism (in the

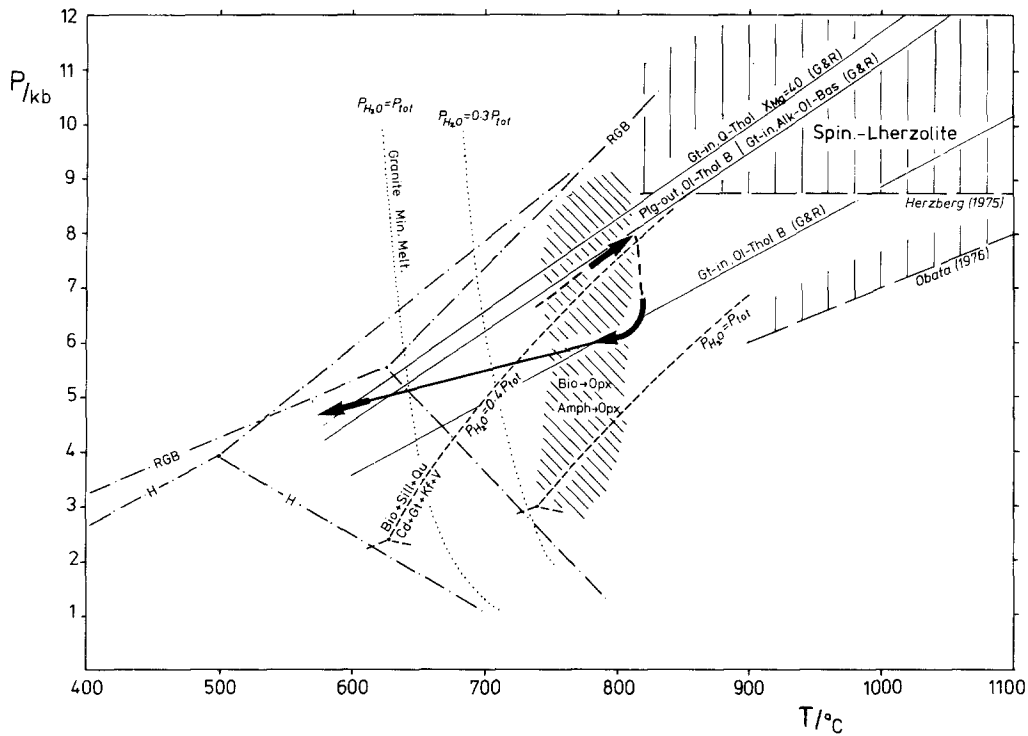


Fig. 11.  $P$ - $T$  path of the granulite-facies rocks of the NW Serre as deduced petrologically from materials of the granulite-pyriclasite unit (Schenk 1978). The pressure decrease during cooling may possibly have been still less than indicated in the figure. Stability of the polymorphs of  $\text{Al}_2\text{SiO}_5$  after Holdaway (1971) (H) and Richardson et al. (1969) (RGB). Curve biotite + sillimanite + quartz = cordierite + garnet + potash feldspar + vapor after Holdaway and Lee (1977). 'Gt-in' and 'Plg-out' curves after Green and Ringwood (1967). Spinel-Lherzolite field after Obata (1976) and Herzberg (1975). Granite minimum melting curves after Kerrick (1972)

granulite-pyriclasite unit about 800°C and 8 kb; Fig. 11) was presumably caused by an uplift of the lower crustal rocks to a level 5 to 7 km higher, where the granulite-facies rocks slowly cooled. Uplift and onset of cooling marking the waning of granulite-facies metamorphism were dated in this work at about 295 m.y. According to the petrological data the cooling has been accompanied only by a small, additional pressure decrease, thus implying that no substantial further uplift occurred.

The sequence of younger sedimentary strata in Calabria is in line with the evolution of the basement as discussed above. The oldest non metamorphic sediments overlying the Palaeozoic phyllites in Southern Calabria are of Jurassic age. Görler (1978) estimates the rock thickness eroded before the Jurassic transgression as about 7 km. From the slow undisturbed shallow water sedimentation in the SE part of the Serre during Mesozoic time, Ergenzinger et al. (1978) postulate a stable hinterland without uplift during this period of time.

Moreover, thick terrestrial sediments of the Oligocene to Miocene, outcropping along the east coast of Southern Calabria, have an increasing inclination with increasing age. This indicates a still later uplift

preferentially of the central and western parts of Southern Calabria (Görler 1978). This last uplift and tilting of the former lower crust of South Calabria during the upper Tertiary, as indicated by erosion and sedimentation, has not yet been dated radiometrically.

The mineral dates presented here do not exclude an interpretation propounding a post-Hercynian reheating and/or a cooling of the basement by uplift during the lower Cretaceous, as advanced by Borsi et al. (1976) to explain the young biotite ages of the basement rocks. However, the model presented here, which involves Hercynian metamorphism and uplift followed by slow cooling in the middle crust, seems to account better for the continuous succession of mineral dates, ranging from 295 to 110 m.y., as well as the petrologically deduced  $P$ - $T$  path and the geodynamic evolution of Southern Calabria.

A more complete model of the Hercynian geodynamic evolution of Southern Calabria should also take into account the extensive plutonic magmatism, which has been shown to be of the same age as the uplift of the lower crust into a higher crustal level. In absence of Rb-Sr whole-rock isochrones, the initial ratios of the tonalite, the quartz dioritic gneiss, and the metamorphosed quartz monzogabbriorite were

estimated by recalculating their  $^{87}\text{Sr}/^{86}\text{Sr}$  ratios back to 300 m.y. The resulting ratios of about 0.710 to 0.711 favour a crustal origin of all these magmatic rocks. In an attempt to find source rocks in the lower crust from which the tonalite, the quartz dioritic gneiss, and the quartz monzogabbronite may have originated by anatexis, one comes up against the difficulty of the high initial ratios (between 0.715 and 0.720) of the granulites and the migmatitic metapelites (Table 2). Moreover, the leucosomes in these rocks are rich in potash feldspar, i.e. not of tonalitic composition. Otherwise, the metabasites of the lower crust, which could act as source rocks of anatectic melts with low  $^{87}\text{Sr}/^{86}\text{Sr}$  ratios, do not show signs of intensive anatexis. As the outcropping lower crustal rocks cannot be regarded as the source for the tonalitic, quartz dioritic, and quartz monzogabbronitic magmatism, the source region must have been situated either below the original position of the granulite-pyriclasite unit, or in the middle crust, which is missing in the outcropping crustal section of Southern Calabria. In the first case, it means that crustal levels still existed below 25 to 30 km; in the latter case, it is necessary to suppose that the anatexis was strongly favored in the middle crust rather than in the lower crust, probably because of a higher water fugacity. Unfortunately, the hypothesis of melting in the middle crust does not help to solve the problem of the relatively low initial ratios of the tonalite and the quartz diorite. Thus further data are still needed in order to construct a well-founded model of the genesis of tonalitic magmatism in Southern Calabria.

### 5.2. *A Comparison with the Granulites of the Ivrea Zone of the Alps and of the Hercynian Belt of Central Europe*

The radiometric ages discussed here are directly comparable with those of the Ivrea and Ceneri Zones in the Southern Alps. In the Ivrea Zone the granulite-facies metamorphism ended also after a Hercynian event, which is dated with  $295 \pm 5$  m.y. by discordant zircons and concordant monazites (Köppel 1974). The oldest inherited zircon population of the Ivrea Zone rocks has a minimum age of about 1,900 m.y. (Köppel 1974) which is identical with the Calabrian zircon ages. Such ages are also known from the Silvretta and Gotthard basement rocks of the Alps (Grauert and Arnold 1968). Furthermore, in the Ivrea-Ceneri Zone and in the Serre, mineral ages diminish towards the higher metamorphic, stratigraphically lower part of the profile (Köppel 1974). In both regions these age differences can be explained by slower cooling of the deeper and hotter parts of the lower crust

relative to higher units, but the cooling of the lower crust in the Serre was altogether slower than in the Ivrea Zone. This picture is further supported by the fact that the Rb-Sr closing temperature of biotite (about  $300^\circ\text{C}$ , after Jäger et al. 1967) was reached in the Serre during the further cooling only at about 135 m.y. (upper part) or at about 110 m.y. (lower part), whereas the biotite ages in the Ivrea Zone range between  $184 \pm 15$  and  $157 \pm 8$  m.y. (Jäger et al. 1967; Graeser and Hunziker 1968; Hunziker 1974). Using zircon, monazite, and biotite ages from a chosen sample locality in the Ivrea Zone (Köppel 1974: ANZ 1; Graeser and Hunziker 1968: KAW 447-54), a cooling curve can be drawn in comparison with the tentative cooling path of the basement of the Serre (Fig. 10).

In addition to the similarities concerning the age of metamorphism and cooling, there are further geological correlations between the Ivrea Zone and the NW Serre. The important fault zone in the Serre, along which the lower crustal rocks were overthrust to the North (Curinga-Girifalco line, Fig. 2), and other alpine mylonitic zones inside the lower crustal unit extend subparallel to the fold axes developed pre- to synmetamorphically in the granulite-pyriclasite unit (Schenk 1978). Correspondingly, the Insubric line is subparallel to the anticlinal axis of the Ivrea crystalline basement (Schmid 1967). In the Ivrea Zone as well as in the Serre thick continuous sequences consisting of deep crustal rocks are overlain by rocks of lower metamorphic grade and by late Hercynian granitoids. In both areas the sedimentation of the transgressive Mesozoic terrains was slow and undisturbed (Bernoulli 1972; Görler 1978).

The overall crustal structures of the two regions with crustal duplications and wave velocity inversions at a depth of about 20–25 km are similar as well (German Research group for explosion seismology, 1968; Schütte 1978). But in contradistinction to the Southern Alps, there is apparently no connection in Southern Calabria between the lower crustal rocks at the surface and a present crust-mantle boundary. This could result from different directions of subduction in Calabria during the Alpine ('Africa-vergent') and during the Apennine ('Europe-vergent') orogeneses (Giese and Görler 1974; Görler and Giese 1978; Amodio-Morelli et al., in press).

Both Calabria and the Ivrea Zone occupy today similar positions at the boundary of the Adriatic microplate, as both lie in sharp bends of the Alpine-Apennine-Maghrebide systems (Fig. 1). Considering all the similarities in the geological evolution mentioned above, one is tempted to compare also their palaeogeographical positions. As deep-seated faults were active in both areas at least since late Hercynian

time, the possibility arises that these faults belong to a common old fault system possibly representing a precursor of the boundary of the Adriatic microplate, both in the Southern Alps and Calabria.

Additionally, one may speculate whether the uplift of the lower crust which began at least in Hercynian time, according to the radiometric dates from the Ivrea Zone and from Southern Calabria, could be correlated with a crustal overlapping between the Adriatic and the European plates; that would mean that the plate boundary which, according to geodynamic models (Giese and Reutter 1978), experienced a crustal overlapping during the Alpine and Apennic orogenies, could have already worked in a similar way as early as the end of the Carboniferous.

The Calabrian granulites experienced a significantly different geological history than the Central European granulites, at least since the Caledonian orogeny, despite striking geological and petrographical similarities. In Central Europe the granulite bodies may have been uplifted from their lower crustal position after the Caledonian granulite-facies metamorphism, reaching the surface at the end of Hercynian time (Jäger and Watznauer 1969; Behr 1978). In contrast, the granulites of Calabria and the Southern Alps, which were possibly situated along the southern border of the Hercynian belt reworked during the Alpine orogeny, remained under granulite-facies conditions in the lower crust until the end of Hercynian time. Uplift to the surface occurred during the Alpine and Apennine orogenies.

*Acknowledgements.* The subject of this study developed from the author's doctoral thesis performed under the supervision of W. Schreyer. The isotopic age determinations were carried out at the Zentrallaboratorium für Geochronologie at Münster (ZLG) under the guidance and advice of B. Grauert. The author gratefully acknowledges assistance during the analytical work from the laboratory staff at Münster, especially from the late A.B. Blaxland, P.J. Patchett, and W. Todt. Sincere thanks are also due to U. Zinkernagel, Bochum, for the cathodoluminescence photographs. The work greatly benefited from discussions and manuscript reviews by W. Todt, B. Grauert, G. Van Kooten, D. Lattard, G. Pritchard and W. Schreyer. This research was supported by the Deutsche Forschungsgemeinschaft, Bonn.

## References

- Alvarez, W.: A former continuation of the Alps. *Geol. Soc. Am. Bull.* **87**, 891–896 (1976)
- Amodio-Morelli, L., Bonardi, G., Colonna, V., Dietrich, D., Giunta, G., Ippolito, F., Liguori, V., Lorenzoni, S., Paglionico, A., Perrone, V., Piccarreta, G., Russo, M., Scandone, P., Zanettin-Lorenzoni, E., Zupetta, A.: L'arco Calabro-Peloritano nell'orogene Apenninico-Maghrebide. *Mem. Soc. Geol. It.* (in press)
- Arnold, A., Scharbert, H.G.: Rb-Sr Altersbestimmungen an Granuliten der südlichen Böhmisches Masse in Österreich. *Schweiz. Mineral. Petrogr. Mitt.* **53**, 61–78 (1973)
- Behr, H.J.: Subfluenz-Prozesse im Grundgebirgs-Stockwerk Mitteleuropas. *Z. dt. geol. Ges.* **129**, 283–318 (1978)
- Bernoulli, D.: North Atlantic and Mediterranean Mesozoic facies: a comparison. In: Initial reports of the Deep Sea Drilling Project Vol. 11, pp. 801–871. Washington: US Government Printing Office 1972 (quoted from Hunziker, 1974)
- Borsi, S., Dubois, R.: Données géochronologiques sur l'histoire hercynienne et alpine de la Calabre Centrale. *C.R. Acad. Sci. [D] (Paris)* **266**, 72–75 (1968)
- Borsi, S., Hieke-Merlin, O., Lorenzoni, S., Paglionico, A., Zanettin-Lorenzoni, E.: Stilo unit and "dioritic-kinzigitic" unit in le Serre (Calabria, Italy). Geological, petrological, geochronological characters. *Boll. Soc. Geol. It.* **95**, 219–245 (1976)
- Cameron, A.E., Smith, D.H., Walker, R.L.: Mass spectrometry of nanogram-size samples of lead. *Anal. Chem.* **41**, 525–526 (1969)
- Ergenzinger, P., Görler, K., Ibbeken, H., Obenauf, P., Rumohr, J.: Calabrian arc and Ionian sea: vertical movements, erosional and sedimentary balance. In: Alps, Apennines, Hellenides (H. Closs, D. Roeder, and K. Schmidt, eds.), pp. 359–373. Stuttgart: Schweizerbart 1978
- Ferrara, G., Longinelli, A.: Età di due rocce granitiche della zona delle Serre in Calabria. *Boll. Geol. Soc. It.* **80**, 25–36 (1961)
- German research group for explosion seismology: Topographie des 'Ivrea-Körpers' abgeleitet aus seismischen und gravimetrischen Daten. *Schweiz. Mineral. Petrogr. Mitt.* **48**, 235–246 (1968)
- Giese, P., Görler, H.: Zur Stellung Kalabriens im geodynamischen Bauplan Italiens. *Nachr. dt. geol. Ges.* **9**, 67–77 (1974)
- Giese, P., Reutter, K.-J.: Crustal and structural features of the margins of the Adria microplate. In: Alps, Apennines, Hellenides (H. Closs, D. Roeder, and K. Schmidt, eds.), pp. 565–588. Stuttgart: Schweizerbart 1978
- Görler, K.: Critical review of postulated nappe structures in Southern Calabria. In: Alps, Apennines, Hellenides (H. Closs, D. Roeder, and K. Schmidt, eds.), pp. 349–354. Stuttgart: Schweizerbart 1978
- Görler, K., Giese, P.: Aspects of the evolution of the Calabrian arc. In: Alps, Apennines, Hellenides (H. Closs, D. Roeder, and K. Schmidt, eds.), pp. 374–388. Stuttgart: Schweizerbart 1978
- Graeser, S., Hunziker, J.C.: Rb-Sr and Pb Isotopen Bestimmungen an Gesteinen und Mineralien der Ivrea Zone. *Schweiz. Mineral. Petrogr. Mitt.* **48**, 189–204 (1968)
- Grauert, B.: U-Pb systematics in heterogeneous zircon populations from the Precambrian basement of the Maryland Piedmont. *Earth Planet. Sci. Lett.* **23**, 238–248 (1974)
- Grauert, B., Arnold, A.: Deutung diskordanter Zirkonalter der Silvretta und des Gotthardmassivs (Schweizer Alpen). *Contrib. Mineral. Petrol.* **20**, 34–56 (1968)
- Grauert, B., Hännly, R., Soptrajanova, G.: Geochronology of a polymetamorphic and anatexitic gneiss region: the Moldanubium of the area Lam-Deggendorf, Eastern Bavaria, Germany. *Contrib. Mineral. Petrol.* **45**, 37–63 (1974)
- Grauert, B., Wagner, M.E.: Age of the granulite-facies metamorphism of the Wilmington complex, Delaware-Pennsylvania Piedmont. *Am. J. Sci.* **275**, 683–691 (1975)
- Green, D.H., Ringwood, A.E.: An experimental investigation of the gabbro to eclogite transformation and its petrological applications. *Geochim. Cosmochim. Acta* **31**, 767–833 (1967)
- Haccard, D., Lorenz, C., Grandjacquet, C.: Essai sur l'évolution tectonogénétique de la liaison Alpes-Apennides (de la Ligurie à la Calabre). *Mem. Soc. Geol. It.* **11**, 309–341 (1972)
- Herzberg, C.T.: Clinopyroxene compositions in spinel-lherzolites. In: Progress in experimental petrology Vol. 3 (G.M. Biggar, ed.), pp. 241–242. London: NERS, Ser. D, No. 6, 1975
- Holdaway, M.J.: Stability of andalusite and the aluminium silicate phase diagram. *Am. J. Sci.* **271**, 97–131 (1971)

- Holdaway, M.J., Lee, S.M.: Fe-Mg Cordierite stability in high-grade pelitic rocks based on experimental, theoretical, and natural observations. *Contrib. Mineral. Petrol.* **63**, 175–198 (1977)
- Hunziker, J.C.: Rb-Sr and K-Ar age determination and the alpine tectonic history of the Western Alps. *Mem. Ist. Geol. Min. Univ. Padova* **31**, 1–55 (1974)
- Jäger, E., Niggli, E., Wenk, E.: Rb-Sr Altersbestimmungen an Glimmern der Zentralalpen. *Beitr. Geol. Karte Schweiz N.F.* **134**, 76 S. (1967)
- Jäger, E., Watznauer, A.: Einige Rb-Sr Datierungen an Granuliten des sächsischen Granulitgebirges. *Mber. dtsh. Akad. Wiss.* **11**, 420–426 (1969)
- Kerrick, D.M.: Experimental determination of muscovite + quartz stability with  $P_{\text{H}_2\text{O}} < P_{\text{total}}$ . *Am. J. Sci.* **272**, 946–958 (1972)
- Köppel, V.: Isotopic U-Pb ages of monazites and zircons from the crust-mantle transition and adjacent units of the Ivrea and Ceneri zones (Southern Alps, Italy). *Contrib. Mineral. Petrol.* **43**, 55–70 (1974)
- Köppel, V., Grünenfelder, M.: Concordant U-Pb ages of monazites from the central Alps and the timing of the high temperature Alpine metamorphism, a preliminary report. *Schweiz. Mineral. Petrogr. Mitt.* **55**, 129–132 (1975)
- Krogh, T.E.: A low-contamination method for hydrothermal decomposition of zircon and extraction of U and Pb for isotopic age determination. *Geochim. Cosmochim. Acta* **37**, 485–494 (1973)
- Obata, M.: The solubility of  $\text{Al}_2\text{O}_3$  in orthopyroxene in spinel and plagioclase peridotites and spinel pyroxenites. *Am. Mineral.* **61**, 804–816 (1976)
- Pidgeon, R.T., Aftalion, M.: The geochronological significance of discordant U-Pb ages of oval-shaped zircons from a Lewisian gneiss from Harris, Outer Hebrides. *Earth Planet. Sci. Lett.* **17**, 269–274 (1972)
- Quitow, H.W.: Der Deckenbau des kalabrischen Massivs und seiner Randgebiete. *Abhand. Gesell. der Wissensch. zu Göttingen*, III. Folge **13**, 63–179 (1935)
- Richardson, S.W., Gilbert, M.C., Bell, P.M.: Experimental de-termination of kyanite-andalusite and andalusite-sillimanite equilibria: the aluminium silicate triple point. *Am. J. Sci.* **267**, 259–272 (1969)
- Schenk, V.: Metamorphe Entwicklung des Altkristallins in der NW-Serre, kalabrisches Massiv, Süd-Italien. *Nachr. dt. geol. Ges.* **17**, 28–29 (1977)
- Schenk, V.: Granulitfazielle Metamorphose in der nordwestlichen Serre, kalabrisches Massiv (Süd-Italien): Geologie und Petrologie. *Diss., Ruhr-Universität Bochum*, 262 S. (1978)
- Schenk, V., Schreyer, W.: Granulite-facies metamorphism in the Northern Serre, Calabria, Southern Italy. In: *Alps, Apennines, Hellenides* (H. Closs, D. Roeder, and K. Schmidt, eds.), pp. 341–346. Stuttgart: Schweizerbart 1978
- Schmid, R.: Zur Petrographie und Struktur der Zone Ivrea-Verbano zwischen Valle d'Ossola und Val Grande (Prov. Novara, Italien). *Schweiz. Mineral. Petrogr. Mitt.* **47**, 935–1118 (1967)
- Schütte, K.-G.: Crustal structure of Southern Italy. In: *Alps, Apennines, Hellenides* (H. Closs, D. Roeder, and K. Schmidt, eds.), pp. 315–320. Stuttgart: Schweizerbart 1978
- Schwarz, G.: Magnetic measurements in Northern Calabria. In: *Alps, Apennines, Hellenides* (H. Closs, D. Roeder, and K. Schmidt, eds.), pp. 321–323. Stuttgart: Schweizerbart 1978
- Steiger, R.H., Jäger, E.: Subcommittee on geochronology: convention on the use of decay constants in geo- and cosmochronology. *Earth Planet. Sci. Lett.* **36**, 359–362 (1977)
- Wagner, G.A., Reimer, G.M., Jäger, E.: Cooling ages derived by apatite fission-track, mica Rb-Sr and K-Ar dating. The uplift and cooling history of the central Alps. *Mem. Ist. Geol. Min. Univ. Padova* **30**, 27 pp. (1977)
- Wetherhill, G.W.: Discordant Uranium-Lead ages. *Trans. Am. Geophys. Union* **37**, 320–326 (1956)
- York, D.: Least-squares fitting of a straight line with correlation errors. *Earth Planet. Sci. Lett.* **5**, 320–324 (1969)

Received January 8, 1979; Accepted March 3, 1980